ECS Transactions, 45 (4) 15-20 (2012)
10.1149/1.3700448 ©The Electrochemical Society

Current Switching in Crossed Graphene Nanoribbons

Roger K. Lake and K. M. Masum Habib

Department of Electrical Engineering, University of California Riverside, Riverside, CA 92521, USA

Current switching by voltage control of the quantum phase has been demonstrated theoretically in crossed graphene nanoribbons. Notable features are the large suppression of the transmission over a wide range of energy of 1.2 eV at zero bias and the high sensitivity of the transmission to an applied bias, changing by 3 orders of magnitude with a bias change of 0.15 V. The magnitude of the current is modulated by a factor of 1000. The area of the intersection that is the active region of the device is 1.8nm x 1.8nm consisting of 120 atoms.

Introduction

Interest in twisted, or misoriented, layers of graphene was recently motivated by the need to understand the electronic properties of multilayer graphene furnace-grown on the C-face of SiC (1). Experimental analysis showed that the layers tended to be rotated with respect to each other at certain angles corresponding to allowed growth orientations with respect to the SiC substrate (2). Density functional theory calculations for such rotated bilayers found that the linear dispersion near the K-points was identical to that of single layer graphene (2). Thus, the rotation was found to be the cause of the decoupling, and the electronic states of the rotated layers of bilayer graphene were the same as those in isolated single-layer graphene. This picture was refined in a following study that found that for twist angles greater than ~3^o, the low-energy carriers behave as massless Dirac Fermions and that for twist angles greater than 20^o, the layers are effectively decoupled and act as independent layers of single-layer graphene (3). Theoretically, calculations of the density of states of randomly stacked graphene layers were first reported in 1992 (4). The more recent work has focused on calculating the energy-wavevector relation as a function of rotation angle using density functional theory (1,2,5,6,7), empirical tight binding (7,8), and continuum models (9). These studies agree that the misaligned graphene bilayers have a linear dispersion for any rotation greater than a few degrees. Very recently there have been studies of the effect of an applied vertical electric field (7,10). There has been one calculation of conduction between two rotated graphene sheets using a pi-bond model and a transfer Hamiltonian expression for current between the two layers (11). This study found the conductance to be enhanced at commensurate angles with relatively small unit cells.

Our work was initially motivated by a curiosity to understand the current-voltage (I-V) relation of two, independently contacted, overlapping, sheets of graphene (12,13,14). We initially considered two collinear armchair graphene nanoribbons (aGNR) 14 C-atoms wide (~1.8nm) with about the same length of overlap (12). The overlap region was arranged in both AB and AA stacking. The width was chosen as 3n+2 to minimize the

bandgap. For these GNRs, the bandgap is 130 meV. As bias was applied, the I-V curve exhibited a peak and region of negative differential resistance.

We next considered two aGNRs crossed at right angles as shown in Fig. 1. In this configuration, the overlap region is neither AB nor AA stacking. For two infinite sheets, a 90^o rotation is the same as a 30^o rotation, which is not a commensurate rotation angle. The Moiré pattern can be observed at the intersection of the two nanoribbons in Fig. 1. The GNRs were terminated a few nanometers after the overlap region. In this crossed configuration, two current peaks were observed in the voltage region between 0 and 0.75 V. Furthermore, the peak-to-valley current ratios were rather large, 13 for the first peak and 7 for the second (14,15). This nonlinear I-V relation with multiple current peaks attracted the attention of circuit designers for applications in high-density functional circuits (15,16). The multiple current peaks were the result of the finite stub effects similar to stub effects in transmission line or waveguide theory. Electronic waves are reflected back from the cut ends giving rise to resonances and anti-resonances as a function of energy. Further, unpublished calculations by us show that the voltage spacing of the current peaks is decreased by increasing the length of the stubs. This is what one would expect viewing the finite ends as resonant cavities.

Infinite Crossed GNRs

However, we were ultimately interested in understanding the current-voltage relation of two infinite, crossed GNRs where finite length effects played no role. This configuration seemed closer to something that might be feasible to build experimentally. Numerically, we converted the finite ends into infinite leads by applying self-energies at all four GNR ends shown in Fig. 1 (numerical details are provided below). The physics governing the charge transport in this system is very different from the physics of the finite crossbars described above.

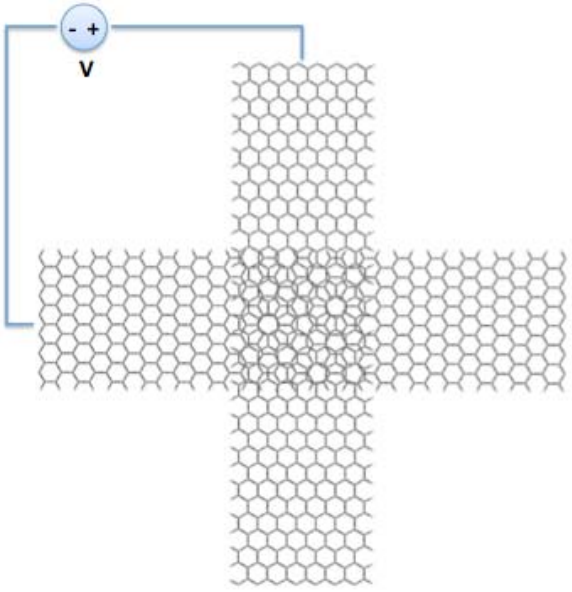

Figure 1. Graphene nanoribbon crossbar.

When the two infinite GNRs are at the same potential, they are effectively decoupled electronically. On a linear scale, the decoupling appears to be perfect. The eigenenergies at the bandedges at Γ ($k_x = k_y = 0$) are doubly degenerate. Plots of the two corresponding eigenstates show one with all of its weight on the top GNR and the other on the bottom GNR. The amount of decoupling can be better determined by looking at the transmission coefficient on a log scale as shown in Fig. 2. There are several things to note. The zero of

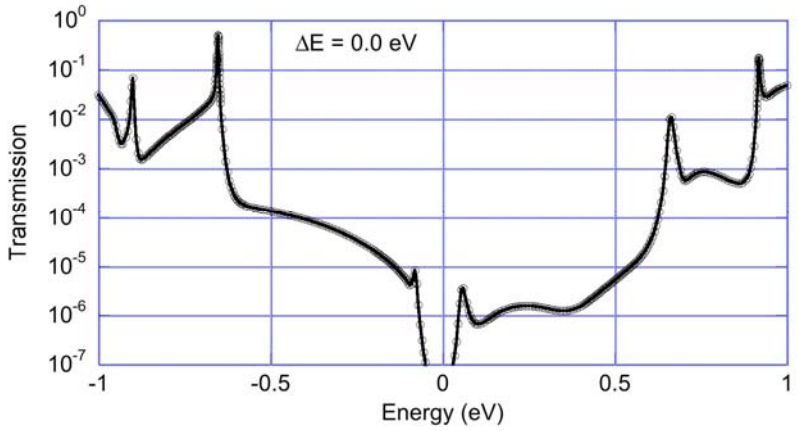

Figure 2. Transmission as a function of energy when the GNRs are at the same potential. All calculated points are shown. The Fermi level is set to E=0. The dip around E=0 corresponds to the 130 meV bandgap of the GNRs.

the energy scale corresponds to the Fermi level. The deep dip in transmission around E=0, corresponds to the 130 meV bandgap of the two GNRs. The transmission is strongly suppressed in the energy range of -0.7 eV < E < 0.7 eV. This is the energy range where there is only one mode propagating in each GNR. At E = ± 0.7 eV, the first excited mode turns on. Then there is significant coupling between the first-excited and the fundamental mode of the top and bottom GNRs. However, over a very large energy range of 1.6 eV (|E| < 0.8 eV), the transmission is suppressed by approximately 3 orders of magnitude. This suppression is the result of destructive quantum interference of the top and bottom wavefunctions. This was shown to be the decoupling mechanism for misoriented two-dimensional sheets of graphene (6), and we have explicitly demonstrated that destructive phase interference is the physical mechanism for the decoupling and suppression of the transmission for the crossed GNRs.

As the potential difference ΔE between the GNRs is increased, the transmission in the low-energy region increases rapidly with ΔE. Fig. 3 shows the transmission with ΔE = 150 meV. The transmission in the low energy region has increased by 3 to 4 orders of magnitude. Again, this is purely the result of the change in the phase of one wavefunction with respect to the other.

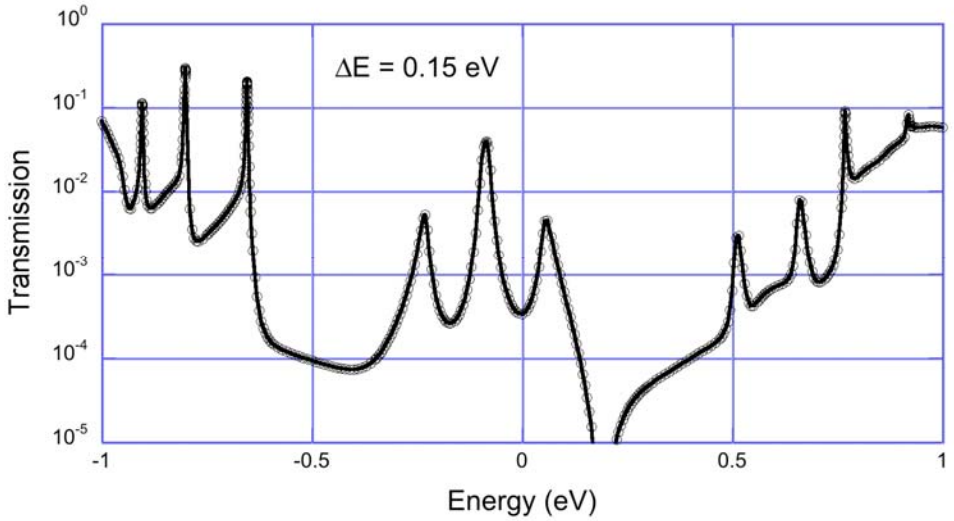

Figure 3. Transmisison when the potential of the top GNR is lowered by 0.15 eV with respect to the bottom GNR.

This sensitivity of the transmission to the energy difference of the two GNRs can be exploited with a built-in potential between the two GNRs. If we start with two GNRs that form a pn junction and apply a voltage as shown in Fig. 1, the applied bias will drive the two GNRs to equal potential. At that point the transmission will turn off. Calculation of the current voltage with an intial built-in potential of 0.25 eV results in the I-V curve shown in Fig. 4. At V=0.25 V, the potential between the two GNRs is driven to zero, and the current shuts off. The peak-to-valley current ratio is 1060.

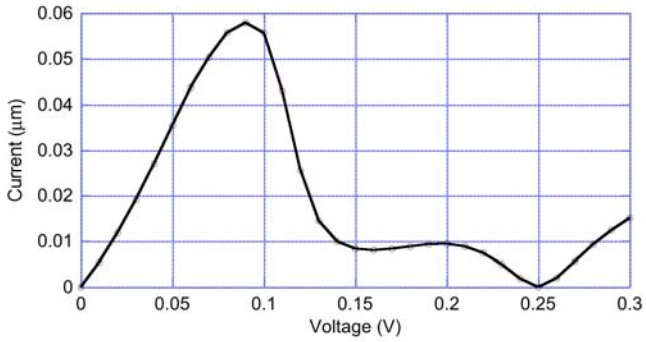

Figure 4. Current-voltage response of crossed graphene nanoribbons with a built-in potential of 0.25 eV.

As we mentioned above, we have explicitly shown that the mechanism of current switching is voltage control of the quantum phase of the wavefunctions. To show this we have calculated the current from a transfer Hamiltonian expression

$$I = \frac{4\pi e}{\hbar}\sum_{m,n}\int dE\left|M_{n,m}\right|^2 N_{1D}^{m}(E)\,N_{1D}^{m}(E-U)\left[f(E-\mu)-f(E-\mu-U\right] \qquad [1]$$

where m and n designate the individual bands of the individual GNRs, N_{1D}^{i} is the 1D density of states of band i, f is the Fermi-dirac distribution, $U=eV$ is potential energy due to the bias, and $M_{n,m}=\left\langle \psi_n(k_y)\middle|H_{\text{int}}\middle|\psi_m(k_x)\right\rangle$ is the matrix element between the state

$|\psi_n(k_y)\rangle$ of the top GNR and the state $|\psi_m(k_x)\rangle$ of the bottom GNR. The matrix element can be decomposed into four components, $M = M_{AA} + M_{AB} + M_{BA} + M_{BB}$, where M_{AA} is the coupling between all the A atoms on the bottom GNR and all the A atoms on the top GNR and so on. The wavefunctions used for evaluating the matrix element are the analytical expressions derived in Ref. (17). We found that the interactions between the A atoms of one GNR with the B atoms of the other GNR are very weak compared to the interaction between the A(B) atoms of one GNR with the A(B) atoms of the other GNR. Thus, the value of the matrix element squared in Eq. [1] is solely a function of the M_{AA} and M_{BB} matrix elements. At zero bias M_{AA} and M_{BB} have equal magnitude but opposite sign making the resultant matrix element (M) very small. This leads to a strong suppression of the transmission at zero bias. This suppression is entirely the result of phase cancellation of the matrix element. At a higher bias, e. g., V= 0.25 V, the phase of M_{BB} is modified by the phase difference between the electronic wave functions of the B atoms of the individual GNRs. This phase difference is caused by the external bias. As a result, the two terms M_{AA} and M_{BB} no longer cancel, the total matrix element is no longer small, and the transmission is no longer suppressed. This analysis confirms that current switching is the result of voltage control of quantum phases.

Numerical Methods

Density functional theory as implemented in FIREBALL combined with a non-equilibrium Green function algorithm were used to calculate the transmission and I-V curves in Figs. 2-4. The details are the same as those described in Ref. (12). In calculating the I-V curve in Fig. 4, all of the applied potential is assumed to drop between the two GNRs. This makes sense from the point of view of a resistive voltage divider. The transmission of an ideal GNR is 1.0, whereas the transmission of the crossed GNRs in the region near the Fermi level is several orders of magnitude lower. Thus, the inter-GNR transfer is the rate-limiting step in the current flow, so that the crossing point is where the voltage will drop. We have repeated these calculations with a Huckel model that reproduces all of the features seen in the DFT results.

Conclusion

We have demonstrated current switching by voltage control of the quantum phase. Notable features are the large suppression of the transmission over an energy range of 1.2 eV at zero bias, and the high sensitivity of the transmission to an applied bias, changing by 3 orders of magnitude with a bias of 0.15 V. The current is modulated by a factor of 1000. The area of the intersection that is the active region of the device is 1.8nm x 1.8nm consisting of 120 atoms. This length scale is below any scale forseen in the ITRS Roadmap.

Acknowledgments

This work is supported by the Microelectronics Advanced Research Corporation Focus Center on Nano Materials (FENA).

References

1. X. Wu, X. Li, Z. Song, C. Berger, and W. A. de Heer, *Phys. Rev. Lett*., **98**, 136801 (2007).
2. J. Hass, F. Varchon, J. E. Millán-Otoya, M. Sprinkle, N. Sharma, W. A. de Heer, C. Berger, P. N. First, L. Magaud, and E. H. Conrad, *Phys. Rev. Lett*., **100**, 125504 (2008).
3. A. Luican, G. Li, A. Reina, J. Kong, R. R. Nair, K. S. Novoselov, A. K. Geim, and E. Y. Andrei, *Phys. Rev. Lett*., **106**, 126802 (2011).
4. J.-C. Charlier, J.-P. Michenaud, and Ph. Lambin, *Phys. Rev. B*, **46**, 4540 (1992).
5. S. Latil, V. Meunier, and L. Henrard, *Phys. Rev. B*, **76**, 210402(R), (2007).
6. S. Shallcross, S. Sharma, and O. A. Pankratov, *Phys. Rev. Lett*., **101**, 056803 (2008).
7. L. Xian, S. Barraza-Lopez, and M. Y. Chou, *Phys. Rev. B*, **84**, 075425 (2011).
8. S. Shallcross, S. Sharma, E. Kandelaki, and O. A. Pankratov, *Phys. Rev. B*, **81**, 165105 (2010).
9. J. M. B. Lopes dos Santos, N. M R. Peres, and A. H. Castro Neto, *Phys. Rev. Lett*., **99**, 256802 (2007).
10. E. S. Morell, P. Vargas, L. Chico, and L. Brey, *Phys. Rev. B*, **84**, 195421 (2011).
11. R. Bistritzer and A. H. MacDonald, *Phys. Rev. B*, **81**, 245412 (2010).
12. K. M. M. Habib, F. Zahid, and R. K. Lake, *Appl. Phys. Lett*., **98**, 192112 (2011).
13. K. M. M. Habib, S. Ahsan, and R. K. Lake, *Proc. SPIE*, **8101**, 81010Q (2011).
14. K. M. M. Habib and R. K. Lake, p. 109, *69th Annual Device Research Conference (DRC)* (2011).
15. K. M. M. Habib, A. Khitun, A. A. Balandin, and R. K. Lake, p. 86, *2011 IEEE/ACM International Symposium on Nanoscale Architectures (NANOARCH)* (2011).
16. S. Khasanvis, K. M. M. Habib, M. Rahman, P. Narayanan, R. K. Lake, and C. A. Moritz, p. 189, *2011 IEEE/ACM International Symposium on Nanoscale Architectures (NANOARCH)* (2011).
17. H. Zheng, Z. F. Wang, T. Luo, Q. W. Shi, and J. Chen, *Phys. Rev. B*, **75**, 165414 (2007).